Applied Catalysis B: Environmental 162 (2015) 85–92

Contents lists available at ScienceDirect

Applied Catalysis B: Environmental

journal homepage: www.elsevier.com/locate/apcatb

Simultaneous removal of monochloroacetic acid and bromate by liquid phase catalytic hydrogenation over $Pd/Ce_{1-x}Zr_xO_2$

Juan Zhou, Ke Wu, Wenjuan Wang, Yuxiang Han, Zhaoyi Xu, Haiqin Wan, Shourong Zheng*, Dongqiang Zhu

State Key Laboratory of Pollution Control and Resource Reuse, Jiangsu Key Laboratory of Vehicle Emissions Control, School of the Environment, Nanjing University, Nanjing 210023, China

ARTICLE INFO

Article history:
Received 27 March 2014
Received in revised form 18 May 2014
Accepted 23 June 2014
Available online 1 July 2014

Keywords:
Liquid-phase catalytic hydrogenation
CeO_2–ZrO_2 solid solutions
Supported Pd catalysts
Simultaneous reduction of monochloroacetic acid and bromate

ABSTRACT

Palladium catalysts supported on ZrO_2, CeO_2 and CeO_2–ZrO_2 solid solutions were prepared using the deposition–precipitation method, and individual and simultaneous reduction of monochloroacetic acid (MCAA) and bromate by liquid-phase catalytic hydrogenation on these catalysts was investigated. The catalysts were characterized by N_2 adsorption–desorption, X-ray diffraction, measurement of point of zero charge, X-ray photoelectron spectroscopy and CO chemisorption. Characterization results showed that CeO_2–ZrO_2 solid solutions with varied Ce/Zr ratios had nearly identical points of zero charge to those of ZrO_2 and CeO_2. For supported Pd catalysts, the binding energy of Pd $3d_{5/2}$ of Pd/CeO_2 was found to be higher than that of Pd/ZrO_2, indicative of a stronger metal-support interaction in the former. Given a similar Pd loading, Pd dispersion of $Pd/Ce_{1-x}Zr_xO_2$ first increased and then decreased with CeO_2 content, and the highest Pd dispersion was observed on $Pd(0.86)/Ce_{0.8}Zr_{0.2}O_2$. Accordingly, $Pd/Ce_{1-x}Zr_xO_2$ exhibited much higher catalytic activities than Pd/ZrO_2 at a Pd loading amount of around 0.85 wt.%, and the highest activity was identified on $Pd(0.86)/Ce_{0.8}Zr_{0.2}O_2$ for individual reduction of bromate and MCAA. The turnover frequencies of $Pd(0.86)/Ce_{0.8}Zr_{0.2}O_2$ for the reduction of bromate and MCAA were 0.69 and 0.23 s^{-1}, respectively, which were one order of magnitude higher than the supported Pd catalysts previously reported. For the simultaneous reduction of MCAA and bromate, the presence of bromate completely suppressed MCAA reduction on $Pd(0.85)/ZrO_2$, while both MCAA and bromate could be effectively reduced on $Pd(0.86)/Ce_{0.8}Zr_{0.2}O_2$. Additionally, the simultaneous reduction of bromate and MCAA proceeded via a competitive reaction mechanism, and the reduction rate of bromate or MCAA was negatively correlated to the competitor concentration.

1. Introduction

Chlorination is an effective and economical disinfection method, which was widely used in the drinking water supply system. However, a diversity of disinfection by products (DBPs) are concurrently formed through a series of reactions between chlorine and inorganic and organic components in the drinking source water. Among DBPs in chlorinated drinking water, monochloroacetic acid (MCAA) and bromate are commonly identified at $\mu g\,l^{-1}$ level [1–5]. Additionally, both MCAA and bromate are considered to be carcinogenic, mutagenic and hepatotoxic, causing potential risk to human health [6–8]. Numerous treatment methods have been developed to remove the DBPs from drinking water [9–13], among which liquid phase catalytic hydrogenation has been proven to be an efficient and clean method to readily eliminate these micro-contaminants. For example, reductive removal of bromate by catalytic hydrogenation was conducted in different reaction systems [14,15]. Very recently, Zhou et al. [16] demonstrated that complete dechlorination of chlorinated acetic acids could be achieved through catalytic hydrogenation over supported noble catalysts.

The catalytic performance of supported noble metal catalysts was strongly dependent on their structural properties. For example, Chen et al. [14] found that the catalytic activities of Pd catalysts supported on SiO_2, activated carbon (AC), and Al_2O_3 for bromate reduction were closely correlated to the points of zero charge (PZCs) of the supports. Similar results were also observed by Zhou et al. [16]. Alternatively, the metal-support interaction played a crucial role on the catalytic activity of the supported catalyst. Reddy et al. [17] found that Ru/Al_2O_3 prepared by the

* Corresponding author. Tel.: +86 25 89680373; fax: +86 25 89680596.
E-mail address: srzheng@nju.edu.cn (S. Zheng).

http://dx.doi.org/10.1016/j.apcatb.2014.06.041
0926-3373/

deposition–precipitation method displayed a higher catalytic activity due to the presence of a stronger metal-support interaction. In parallel, Gopinath et al. [18] attributed the superior activity and stability of Pd/Al_2O_3 prepared by the deposition–precipitation method to the strong metal-support interaction. Zhou et al. [16] studied the catalytic hydrodechlorination of chlorinated acetic acids over Pd/ZrO_2 and observed similar results. It is worth mentioning that for ZrO_2 supported noble metal catalyst CeO_2 doping may invoke additional metal-support interaction, leading to enhanced metal dispersion and suppressed metal sintering [19].

In previous studies, single contaminant was usually used to test the feasibility of catalytic hydrogenation for the reductive removal of DBPs in drinking water. However, a variety of DBPs commonly coexists in the chlorinated drinking water [20]. It was further reported that the individual reduction of most DBPs was implemented via an adsorption controlled reaction mechanism [14,16]. Nonetheless, little is known about the mechanism of the simultaneous reduction of multiple DBPs. We hypothesize that the simultaneous reduction of DPBs may process via a competitive reaction mechanism, and the reaction competitiveness of DBPs may differ with their structure. To our best knowledge, however, the simultaneous reduction of multiple DBPs has not been conducted thus far.

The main objective of this study is to systematically investigate the simultaneous reduction of MCAA and bromate in water by the catalytic hydrogenation over $Pd/Ce_{1-x}Zr_xO_2$ ($x = 0.2, 0.5, 0.8$). The catalysts were characterized by N_2 adsorption–desorption, X-ray diffraction, measurement of point of zero charge, X-ray photoelectron spectroscopy and CO chemisorption.

2. Experimental

2.1. Catalyst preparation

CeO_2, ZrO_2 and CeO_2–ZrO_2 solid solutions with varied Ce/Zr ratios were prepared using the precipitation/coprecipitation method. For CeO_2 or ZrO_2, 0.1 M ammonia solution was added dropwise to 200 ml of 0.1 M $Ce(NO_3)_3{\cdot}6H_2O$ or $ZrOCl_2{\cdot}8H_2O$ solution under vigorous stirring until pH reached 10.0. After stirring for another 2 h at room temperature, the resulting precipitant was recovered by filtration, followed by washing with distilled water, and drying at 105 °C for 6 h. Then, the samples were calcined at 500 °C in air for 4 h. To prepare CeO_2–ZrO_2 solid solutions with varied Ce/Zr ratios, 100 ml of quantitative solutions containing $ZrOCl_2$ and $Ce(NO_3)_3$ with ratios of $Ce{:}Zr = (1-x){:}x$ ($x = 0.2, 0.5, 0.8$) and total cation concentration of 0.1 M were prepared, which were subjected to the same treatment as CeO_2 and ZrO_2. The resulting CeO_2–ZrO_2 solid solution is referred to as $Ce_{1-x}Zr_xO_2$ ($x = 0.2, 0.5, 0.8$).

Supported Pd catalysts were prepared using the deposition–precipitation method. Briefly, the support was suspended in 30 ml of distilled water, to which a desired amount of $PdCl_2$ solution was added under stirring. Then, 1.0 M Na_2CO_3 solution was used to adjust the solution pH to 10.5. After stirring for 1 h, the catalyst was collected by filtration, followed by repeated washing with distilled water, drying at 105 °C for 6 h, calcining at 300 °C in air for 4 h, and finally reducing at 300 °C under a H_2 stream (40 ml min^{-1}) for 2 h. The resultant catalysts are referred to as $Pd(z)/ZrO_2$, $Pd(z)/CeO_2$ or $Pd(z)/Ce_{1-x}Zr_xO_2$, where z is the Pd loading amount (wt.%). In order to avoid potential intraparticle diffusion effects, all catalysts were ground to pass through a 400-mesh sieve (<37 μm) prior to catalytic activity test [21,22].

2.2. Catalyst characterization

The X-ray diffraction (XRD) patterns were obtained on a Rigaku D/max-RA powder diffraction-meter using a Cu $K\alpha$ radiation (Rigaku, Tokyo, Japan). The Brunauer–Emmett–Teller (BET) surface areas of the samples were determined using N_2 adsorption on a Micromeritics ASAP 2020 instrument (Micromeritics Instrument Co., Norcross, GA, USA) at −196 °C. The Pd contents in the catalysts were detected using an inductive coupled plasma emission spectrometer (ICP) (J-A1100, Jarrell-Ash, USA). The X-ray photoelectron spectroscopy (XPS) was obtained on a PHI5000 Versa Probe equipped with a monochromatized Al $K\alpha$ excitation source ($h\nu = 1486.6$ eV) (ULVAC-PHI, Japan). The C 1s peak (284.6 eV) was used for the calibration of binding energy.

The Pd dispersion of the supported catalyst was determined using the CO chemisorption method. Briefly, 100 mg of reduced catalyst was loaded in a U-shaped quartz tube and was activated in a H_2 stream (40 ml min^{-1}) at 300 °C for 1 h. After purging with an Ar flow (30 ml min^{-1}) at 300 °C for 1 h, the catalyst was cooled down to room temperature. The CO chemisorption was conducted using the pulse titration model and the CO contents in the pulses were monitored using a thermal conductivity detector (TCD). The Pd dispersions and Pd particle sizes of the supported catalysts were calculated assuming average chemisorption stoichiometry of $CO/Pd_{surface} = 1$ [23,24].

The points of zero charge (PZCs) of the supports were determined using the potentiometric mass titration method [25,26]. Briefly, 0.4 g of the support was dispersed in 50 ml of 0.03 M KNO_3 solution at 25 °C. Then, 0.2 ml of 1.0 M NaOH was added into the mixture, which was allowed to equilibrate for 20 h to reach a stable pH. The suspension was titrated by 0.5 M HNO_3 solution under continuous bubbling with a N_2 flow (50 ml min^{-1}). The pH was recorded after each addition of the acidic solution. A blank solution was also titrated according to the above described procedure.

2.3. Liquid phase catalytic hydrogenation reaction

The catalytic activities of supported Pd catalysts were examined under atmospheric pressure of hydrogen in a 500 ml of four-necked flask equipped with a sample port, pH-stat, H_2/N_2 inlet and outlet. The reaction temperature was stabilized at 25 ± 0.5 °C with a water-bath (SDC-6, Scientz Co., China). Briefly, 10 mg of catalyst was added in 300 ml of 0.2 mM MCAA or bromate solution with pH pre-adjusted to 5.6 using 1.0 M NaOH. The mixture was purging using a N_2 flow (50 ml min^{-1}) under vigorous stirring (1400 rpm) for 30 min, then the N_2 flow was switched to a H_2 flow (250 ml min^{-1}) during the reaction process. Samples were taken at selected intervals and the catalyst particles were removed by fast filtration. The concentrations of reactants and products in the filtrate were determined using an Ion Chromatography (ICS1000, Dionex, USA) with a mobile phase of 10 mM KOH solution. The initial activity of the catalyst was calculated based on the first-order rate law at the conversion of MCAA or bromate below 25%. The data reproducibility was confirmed by two separated runs of simultaneous reduction of MCAA and bromate over $Pd(0.86)/Ce_{0.8}Zr_{0.2}O_2$ (results presented in Fig. 1S, supporting information). To test the possible mass transfer limitation, the individual reduction of MCAA and bromate over $Pd(0.86)/Ce_{0.8}Zr_{0.2}O_2$ with varied catalyst dosages was conducted, and the results are shown in Fig. 2S, supporting information. The catalyst dosage normalized activities remained nearly constant for the reduction of MCAA and bromate, indicative of the absence of mass transfer limitation under our experimental conditions.

3. Results and discussion

3.1. Catalyst characterization

The XRD patterns of Pd catalysts supported on ZrO_2, CeO_2, and CeO_2–ZrO_2 solid solutions with varied Ce/Zr ratios are compared

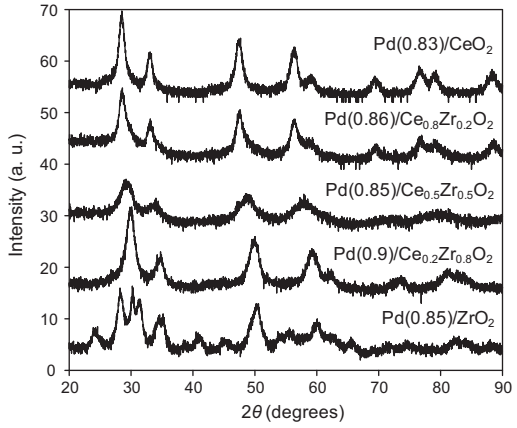

Fig. 1. XRD patterns of Pd catalysts supported on CeO_2, ZrO_2 and $Ce_{1-x}Zr_xO_2$ solid solutions.

Table 1
BET surface areas and points of zero charge of the supports.

Samples	BET surface area ($m^2\ g^{-1}$)	PZC
ZrO_2	83.2	6.3
$Ce_{0.2}Zr_{0.8}O_2$	92.5	6.1
$Ce_{0.5}Zr_{0.5}O_2$	102.3	6.5
$Ce_{0.8}Zr_{0.2}O_2$	94.9	6.2
CeO_2	85.6	6.4

in Fig. 1. For all Pd catalysts, diffraction peaks were clearly identified from catalyst supports, not from either PdO or Pd, likely due to a low Pd content and high Pd dispersion. The main diffraction peaks of ZrO_2 in Pd(0.85)/ZrO_2 were observed with 2θ at 24.2, 28.2, 30.3, 31.5, 34.8, 35.3, 50.2 and 60.0°, indicative of the coexistence of monoclinic and tetragonal ZrO_2 phases [27,28]. For Pd/CeO_2, diffraction peaks were identified at 28.5, 33.0, 47.3, 56.2 and 78°, characteristic of a typical cubic CeO_2 phase with a fluorite structure [29,30]. The XRD patterns of Pd/$Ce_{1-x}Zr_xO_2$ catalysts were analogous to that of CeO_2, indicating that homogeneous CeO_2–ZrO_2 solid solutions with a stable fluorite structure were formed in the tested Ce/Zr ratio range. Notably, the diffraction peaks of $Ce_{1-x}Zr_xO_2$ solid solution shifted to large angles with the increase of ZrO_2 content, reflecting a cell contraction due to the substitution of larger cerium ion by smaller zirconium ion [31,32]. The XRD patterns of Pd catalysts supported on $Ce_{0.8}Zr_{0.2}O_2$ with varied Pd loading amounts are presented in Fig. 3S, supporting information. The diffraction peaks of the catalysts were essentially identical, suggesting that the structure of $Ce_{0.8}Zr_{0.2}O_2$ was stable upon Pd loading.

The surface areas and PZCs of the supports are summarized in Table 1. The surface area of $Ce_{1-x}Zr_xO_2$ first increased and then decreased with CeO_2 content. ZrO_2, CeO_2 and CeO_2–ZrO_2 solid solutions displayed nearly identical PZCs, likely due to the similar PZC of ZrO_2 to that of CeO_2 [33–35].

The XPS spectra of supported Pd catalysts in the Zr 3p and Pd 3d regions are compiled in Fig. 2. Because Pd $3d_{5/2}$ was partially overlapped by Zr $3p_{3/2}$, the XPS profiles were deconvoluted and the results are listed in Table 2. The binding energy of Pd $3d_{5/2}$ of Pd(0.85)/ZrO_2 was found to be 335.5 eV, higher than that of metallic Pd (335.0 eV) [36,37]. Such a higher binding energy can be attributed to the electron transfer from metallic Pd to ZrO_2 support due to a strong metal-support interaction [38]. In comparison, the binding energy of Pd $3d_{5/2}$ of Pd(0.83)/CeO_2 was observed at 337.1 eV, indicative of a much stronger metal-support interaction than that in Pd(0.85)/ZrO_2. Accordingly, increasing CeO_2 content in $Ce_{1-x}Zr_xO_2$ led to an increase in the binding energy of Pd $3d_{5/2}$, as reflected by the results of Pd(0.90)/$Ce_{0.2}Zr_{0.8}O_2$,

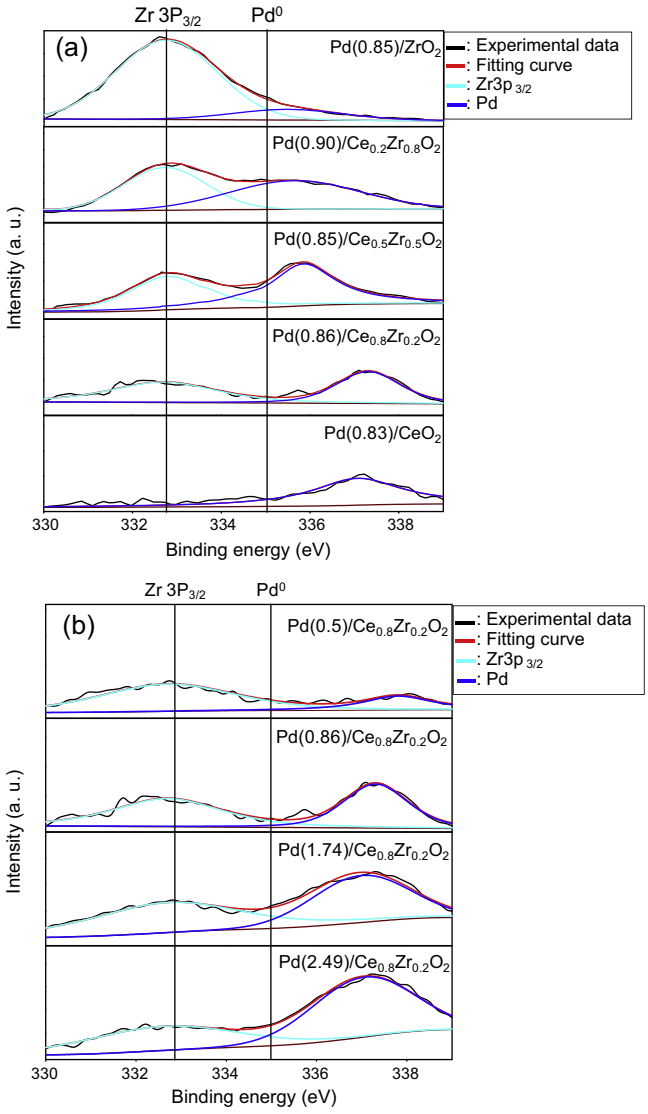

Fig. 2. XPS profiles of (a) Pd catalysts supported on different supports, and (b) Pd/$Ce_{0.8}Zr_{0.2}O_2$ catalysts with varied Pd loadings.

Pd(0.85)/$Ce_{0.5}Zr_{0.5}O_2$ and Pd(0.86)/$Ce_{0.8}Zr_{0.2}O_2$. However, the binding energy of Pd $3d_{5/2}$ in Pd(0.86)/$Ce_{0.8}Zr_{0.2}O_2$ was 337.3 eV, slightly higher than that in Pd(0.83)/CeO_2. Notably, ZrO_2 doping in CeO_2 could enhance the mobility of lattice O of CeO_2, resulting in cationic defects, which may invoke additional metal-support interaction and cationization of metallic Pd [39–41]. The strong metal-support interaction was also observed on Pd catalysts supported on $Ce_{0.8}Zr_{0.2}O_2$ with varied Pd loadings. Increasing Pd loading from 0.50 to 2.49 wt.% resulted in a decrease in the binding energy from 337.8 to 336.9 eV, reflecting an attenuated metal-support interaction with the increase of Pd particle size.

Pd dispersions of supported Pd catalysts were determined using the CO chemisorption method and the results are listed in Table 2. The Pd dispersion initially increased and then decreased with CeO_2 content in $Ce_{1-x}Zr_xO_2$, and the maximum value was observed on Pd(0.86)/$Ce_{0.8}Zr_{0.2}O_2$, confirming a positive impact of the metal-support interaction on Pd dispersion. For Pd/$Ce_{0.8}Zr_{0.2}O_2$, increasing Pd loading amount from 0.50 to 2.49 wt.% led to a decrease of Pd dispersion from 96.0% to 64.2%, reflecting a gradual aggregation of Pd particles on support surface.

The average Pd particle sizes of the catalysts could be quantified based on CO chemisorption data (see results in Table 2). In line with

Table 2
Structural properties of supported Pd catalysts.

Samples	Pd $3d_{5/2}$ (eV)[a]	Pd content (wt.%)[b]	Pd dispersion (%)[c]	Pd particle size (nm)[c]	CO adsorption amount ($\mu mol\,g^{-1}$)[c]
$Pd(0.85)/ZrO_2$	335.5	0.85	60.8	1.84	55.0
$Pd(0.83)/CeO_2$	337.1	0.83	85.4	1.31	66.7
$Pd(0.90)/Ce_{0.2}Zr_{0.8}O_2$	335.6	0.90	70.7	1.59	59.7
$Pd(0.85)/Ce_{0.5}Zr_{0.5}O_2$	335.9	0.85	81.2	1.38	64.9
$Pd(0.50)/Ce_{0.8}Zr_{0.2}O_2$	337.8	0.50	96.0	1.17	44.2
$Pd(0.86)/Ce_{0.8}Zr_{0.2}O_2$	337.3	0.86	90.5	1.24	89.7
$Pd(1.74)/Ce_{0.8}Zr_{0.2}O_2$	337.0	1.74	84.9	1.32	139.0
$Pd(2.49)/Ce_{0.8}Zr_{0.2}O_2$	336.9	2.49	64.2	1.75	150.0

[a] Determined by XPS.
[b] Determined by ICP.
[c] Calculated from CO chemisorption.

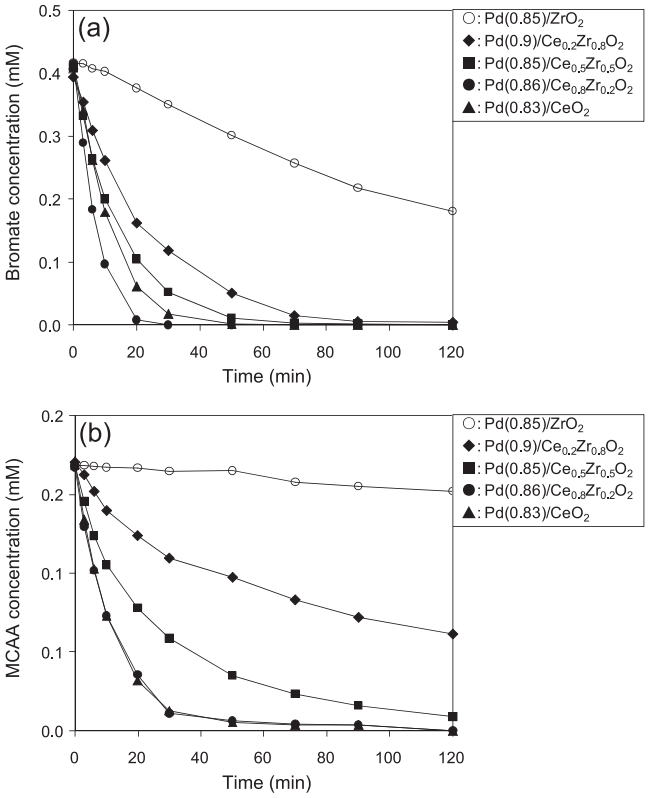

Fig. 3. Catalytic hydrogenation of (a) bromate and (b) MCAA over Pd catalysts supported on different supports. Reaction conditions: pH 5.6, Catalyst dosage: $0.033\,g\,l^{-1}$, initial bromate concentration: 0.41 mM, initial MCAA concentration: 0.17 mM.

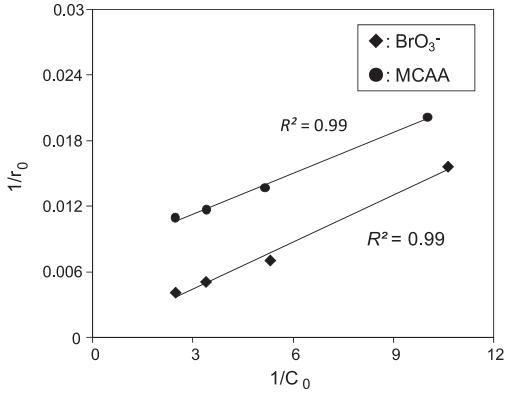

Fig. 4. Linear plots of $1/r_0$ *versus* $1/C_0$ for individual reduction of bromate and MCAA. Reaction conditions: pH 5.6. Catalyst: $Pd(0.86)/Ce_{0.8}Zr_{0.2}O_2$. Catalyst dosage: $0.033\,g\,l^{-1}$. Line represents the fitting curve using the Langmuir–Hinshelwood model.

Pd dispersion, Pd particle size first decreased with CeO_2 content in $Ce_{1-x}Zr_xO_2$ and reached the minimum on $Pd(0.86)/Ce_{0.8}Zr_{0.2}O_2$. The Pd particle size of $Pd(0.83)/CeO_2$ was 1.31 nm, slightly larger than that of $Pd(0.86)/Ce_{0.8}Zr_{0.2}O_2$.

3.2. Individual reduction of bromate and MCAA

3.2.1. Effect of support

The individual reduction of bromate and MCAA over supported Pd catalysts is presented in Fig. 3. For $Pd(0.85)/ZrO_2$, bromate was removed by 56.6% within 120 min of catalytic hydrogenation. Complete bromate reduction could be achieved within 120 min for $Pd(0.9)/Ce_{0.2}Zr_{0.8}O_2$, 90 min for $Pd(0.85)/Ce_{0.5}Zr_{0.5}O_2$ and 30 min for $Pd(0.86)/Ce_{0.8}Zr_{0.2}O_2$, indicating that increasing CeO_2 content in $Ce_{1-x}Zr_xO_2$ significantly enhanced the catalytic activity. In contrast, bromate reduction was completed within 50 min on $Pd(0.83)/CeO_2$, reflecting a slightly lower activity than that of $Pd(0.86)/Ce_{0.8}Zr_{0.2}O_2$. Consistently, the initial activities of $Pd(0.85)/ZrO_2$, $Pd(0.9)/Ce_{0.2}Zr_{0.8}O_2$, $Pd(0.85)/Ce_{0.5}Zr_{0.5}O_2$, $Pd(0.86)/Ce_{0.8}Zr_{0.2}O_2$ and $Pd(0.83)/CeO_2$ were calculated to be 8.1, 79.0, 144.5, 250.5 and 150.3 $mM\,g_{cat}^{-1}\,h^{-1}$, respectively, verifying an activity order of $Pd(0.86)/Ce_{0.8}Zr_{0.2}O_2 > Pd(0.83)/CeO_2 > Pd(0.85)/Ce_{0.5}Zr_{0.5}O_2 > Pd(0.9)/Ce_{0.2}Zr_{0.8}O_2 > Pd(0.85)/ZrO_2$. In parallel, a similar order of catalytic activity was identified for MCAA reduction (see Fig. 3b).

The activity of the supported Pd catalyst is generally linked to the structural properties of both support and superficial Pd particle [42–44]. It was previously reported that in the liquid phase catalytic hydrogenation the activity of supported catalyst differed with the PZC of support [14,16]. For the tested catalysts, the supports (ZrO_2, CeO_2 and $Ce_{1-x}Zr_xO_2$) had nearly identical PZCs (see Table 1). Under the reaction conditions, the catalyst surface was positively charged, favoring the effective hydrogenation reduction by invoking an attractive interaction between the reactant and catalyst. Hence, the variation of catalytic activities is more likely correlated to the structural properties of superficial Pd particles.

Compared with ZrO_2 support, due to CeO_2 doping $Ce_{1-x}Zr_xO_2$ solid solutions may invoke additional metal-support interaction, resulting in decreased Pd particle size and increased Pd dispersion. Accordingly, at a given Pd loading more Pd sites are available on $Pd/Ce_{1-x}Zr_xO_2$ than those on Pd/ZrO_2. Furthermore, XPS results showed that CeO_2 doping enhanced the cationization of superficial Pd particle, which favored the adsorption of anions (bromate and MCAA) onto Pd sites, and the activation of reactants [45,46], giving rise to enhanced catalytic activity. Consistently, significantly enhanced reduction of chloroacetic acids was previously reported due to the presence of a strong metal-support interaction and cationic Pd species in supported Pd catalysts [16].

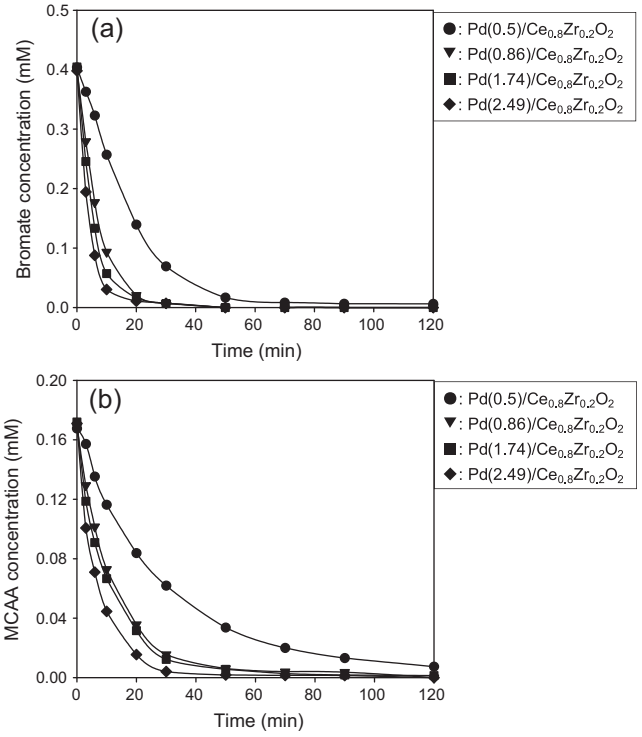

Fig. 5. Catalytic hydrogenation of (a) bromate and (b) MCAA over Pd catalysts with varied Pd loadings. Reaction conditions: pH 5.6, Catalyst dosage: 0.033 g l^{-1}, initial bromate concentration: 0.41 mM, initial MCAA concentration: 0.17 mM.

3.2.2. *Influence of adsorption on individual reduction of bromate and MCAA*

Because the liquid phase catalytic hydrogenation is a heterogeneous reaction process, reactant adsorption is believed to be a prerequisite step. To evaluate the impact of reactant adsorption on the catalytic activity of Pd(0.86)/$Ce_{0.8}Zr_{0.2}O_2$, the catalytic reduction of individual bromate and MCAA with varied initial concentrations was conducted, and the results are presented in Fig. 4S, supporting information. For bromate reduction, increasing initial concentration led to increased reaction rate, implying that the reaction rate is positively correlated to the concentration of bromate adsorbed on catalyst surface. This hypothesis can be further verified by fitting the experimental data to the Langmuir–Hinshelwood model [47,48]:

$$r_0 = k\theta_s = k\frac{bC_0}{1+bC_0} \quad (1)$$

$$\frac{1}{r_0} = \frac{1}{kbC_0} + \frac{1}{k} \quad (2)$$

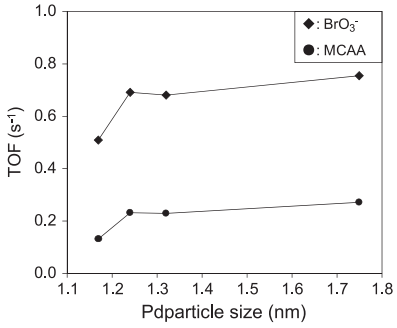

Fig. 6. Initial TOFs of exposed Pd sites in Pd(0.86)/$Ce_{0.8}Zr_{0.2}O_2$ for individual reduction of bromate and MCAA. Reaction conditions: pH 5.6. Catalyst dosage: 0.033 g l^{-1}, initial bromate concentration: 0.41 mM, initial MCAA concentration: 0.17 mM.

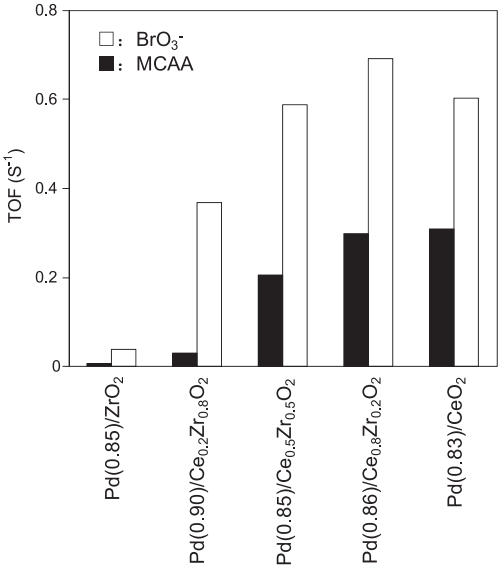

Fig. 7. Initial TOFs of exposed Pd sites in Pd catalysts supported on different supports for individual reduction of bromate and MCAA. Reaction conditions: pH 5.6. Catalyst dosage: 0.033 g l^{-1}, initial bromate concentration: 0.41 mM, initial MCAA concentration: 0.40 mM.

where r_0 is the initial reaction rate, C_0 is the initial reactant concentration in water, θ_s is the surface coverage of reactant adsorption, k is the reaction rate constant, and b is the adsorption constant.

Fig. 4 presents the dependence of initial reaction rate on initial concentration plotted as $1/C_0$ *versus* $1/r_0$. A good linear relationship with R^2 values higher than 0.99 indicated that the individual reduction of bromate and MCAA on Pd(0.86)/$Ce_{0.8}Zr_{0.2}O_2$ follows the Langmuir–Hinshelwood model, confirming an adsorption controlled reaction mechanism. According to the model, the reaction rate constant was calculated to be 285.7 mM g_{cat}^{-1} h^{-1} for bromate reduction, much higher than that of MCAA reduction (128.2 mM g_{cat}^{-1} h^{-1}).

3.2.3. *Effect of Pd loading amount*

The effect of Pd loading amount on the reduction of bromate and MCAA over Pd/$Ce_{0.8}Zr_{0.2}O_2$ catalysts is presented in Fig. 5. For bromate reduction, increasing Pd loading from 0.50 to 2.49 wt.% led to an increase of the initial reaction rate from 82.1 to 407.6 mM g_{cat}^{-1} h^{-1}. In parallel, the initial activity for MCAA reduction increased from 20.8 to 148.6 mM g_{cat}^{-1} h^{-1}. The positive relationship between Pd loading and the catalytic activity could be tentatively attributed to more active sites accessible for the catalyst with a higher Pd loading, as indicated by the CO chemisorption results (see Table 2).

The comparison of the turnover frequency (TOF) of catalytic active site may provide more insights into the dependency of catalytic activity on the structural properties of Pd particle. The TOF was defined as the initial reduction rate of bromate/MCAA per exposed Pd atom, which was calculated based on CO chemisorption data. The results are compiled in Fig. 6. For both MCAA and bromate, the TOF of exposed Pd site first increased and then remained nearly constant with Pd particle size. In principle, H_2 activation and adsorption/activation of reactant are the crucial steps involved in the catalytic hydrogenation reaction [16,46]. A smaller Pd particle is prone to invoking a stronger metal-support interaction and forming more cationized Pd species, favoring the adsorption and activation of anionic reactant (*e.g.* bromate and MCAA), while a larger Pd particle facilitates H_2 activation by forming β-PdH phase. The initially increased catalytic activity with Pd particle size indicates that compared with the adsorption and activation of reactant H_2

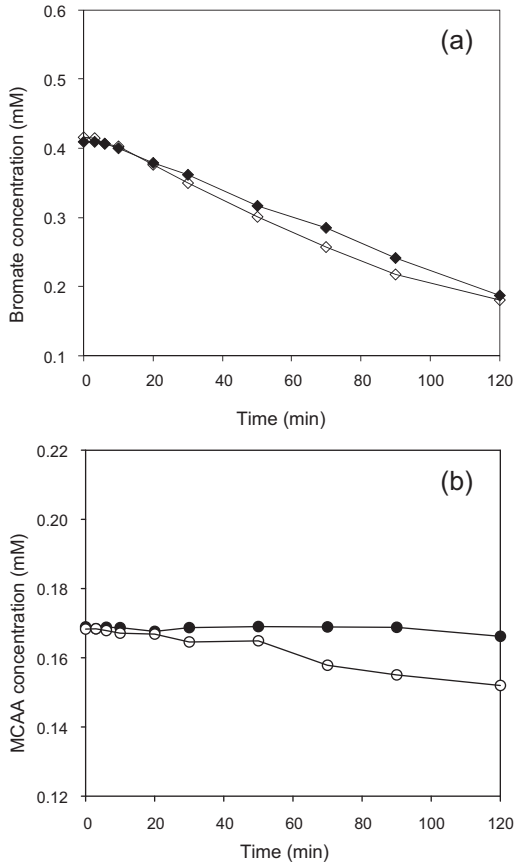

Fig. 8. Individual and simultaneous reduction of bromate and MCAA over Pd(0.85)/ZrO_2. Filled symbols denote simultaneous reduction and open symbols denote individual reduction. Reaction conditions: pH 5.6. Catalyst dosage: 0.033 g l^{-1}, initial bromate concentration: 0.41 mM, initial MCAA concentration: 0.17 mM.

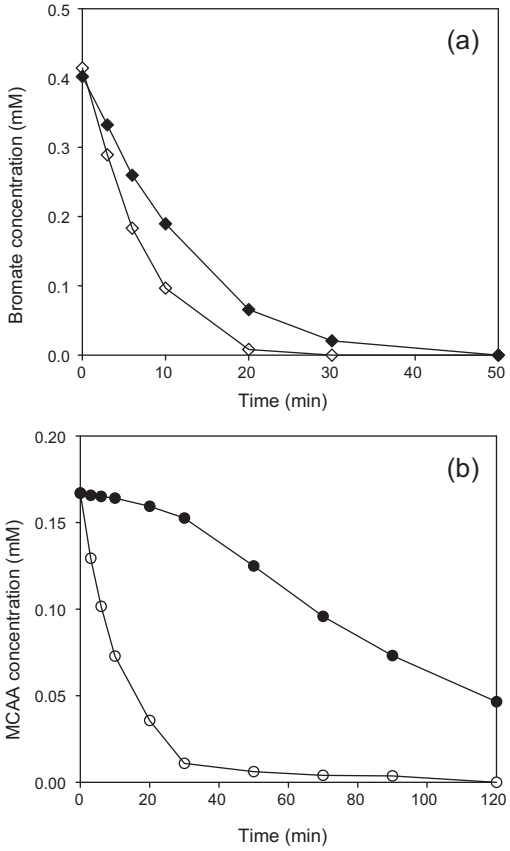

Fig. 9. Individual and simultaneous reduction of bromate and MCAA over Pd(0.86)/$Ce_{0.8}Zr_{0.2}O_2$. Filled symbols denote simultaneous reduction and open symbols denote individual reduction. Reaction conditions: pH 5.6. Catalyst dosage: 0.033 g l^{-1}, initial bromate concentration: 0.41 mM, initial MCAA concentration: 0.17 mM.

activation is a more important rate-controlling step for the supported catalyst with smaller Pd particles, while for the catalysts with relatively larger Pd particles H_2 activation and adsorption/activation of reactant have equal importance. It should be emphasized that under similar reaction conditions the TOF values of exposed Pd sites in Pd(0.86)/$Ce_{0.8}Zr_{0.2}O_2$ were 0.23 and 0.69 s^{-1} for the individual reduction of MCAA and bromate, respectively, which were approximately one order of magnitude higher than those of supported Pd catalysts reported previously [14,16]. Furthermore, the TOF of a given catalyst differed with the reactants (results presented in Fig. 7). For example, the initial TOF values of Pd(0.85)/ZrO_2 were 0.0054 and 0.039 s^{-1} for MCAA and bromate, respectively, reflecting a much lower reactivity of MCAA than that of bromate. Similarly, the higher reactivity of bromate was observed on other catalysts with different supports, implying that MCAA and bromate may display different reaction competitiveness in the simultaneous hydrogenation reduction process.

3.3. Simultaneous reduction of bromate and MCAA

The simultaneous reduction of bromate and MCAA over Pd(0.85)/ZrO_2 and Pd(0.86)/$Ce_{0.8}Zr_{0.2}O_2$ is presented in Figs. 8 and 9, respectively. For comparison purpose, the individual reduction of bromate and MCAA was also included. Compared with individual MCAA reduction the presence of bromate markedly suppressed MCAA reduction on both Pd(0.85)/ZrO_2 and Pd(0.86)/$Ce_{0.8}Zr_{0.2}O_2$. The inhibited MCAA reduction by bromate could be well explained in terms of a competitive adsorption mechanism, by which bromate adsorption on catalyst surface partially blocks the active sites, slowing down MCAA reduction. Consistently, suppressed reaction due to competitive adsorption was observed previously [49–51]. Interestingly, MCAA reduction over Pd(0.86)/$Ce_{0.8}Zr_{0.2}O_2$ was very slow at the initial reaction stage because of competitive bromate adsorption on catalyst surface, and was prominently accelerated after about 30 min of reaction due to nearly complete consumption of bromate (see Fig. 9a), further confirming the marked inhibition of MCAA reduction by the competitive adsorption of bromate.

Notably, bromate and MCAA exhibited different reaction competitiveness on Pd(0.85)/ZrO_2. For example, the presence of 0.41 mM of bromate completely suppressed MCAA reduction. Accordingly, bromate was reduced by 56.6% in the absence of MCAA and by 54.3% in the presence of 0.17 mM MCAA within 120 min of catalytic hydrogenation, reflecting a negligible influence of MCAA adsorption on bromate reduction. Such a stronger competitiveness of bromate is likely due to a much higher adsorption affinity of bromate to the catalyst than that of MCAA. However, the reaction competitiveness of MCAA and bromate differed with the catalysts. In contrast to the complete suppression of MCAA reduction by bromate on Pd(0.85)/ZrO_2, effective and simultaneous reduction of MCAA and bromate could be achieved on Pd(0.86)/$Ce_{0.8}Zr_{0.2}O_2$. Furthermore, the presence of 0.41 mM bromate resulted in a decrease in the initial activity of Pd(0.86)/$Ce_{0.8}Zr_{0.2}O_2$ from 73.2 to 13.0 mM g_{cat}^{-1} h^{-1} for MCAA reduction. In parallel, the presence of 0.17 mM MCAA led to a decrease in the initial activity of Pd/$Ce_{0.8}Zr_{0.2}O_2$ for bromate reduction from 250.5 to 131.4 mM g_{cat}^{-1} h^{-1}. The increased reaction competitiveness of MCAA on Pd(0.86)/$Ce_{0.8}Zr_{0.2}O_2$ is possibly due

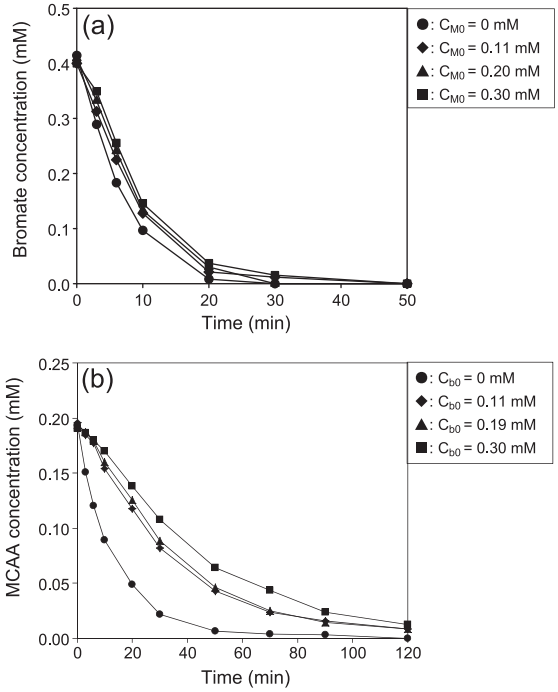

Fig. 10. (a) Influence of MCAA concentration on bromate reduction and (b) influence of bromate concentration on MCAA reduction. Reaction conditions: pH 5.6. Catalyst: Pd(0.86)/$Ce_{0.8}Zr_{0.2}O_2$. Catalyst dosage: 0.033 g l^{-1}.

to enhanced MCAA adsorption on $Ce_{0.8}Zr_{0.2}O_2$, implying that the reactant selectivity could be tuned by adjusting catalyst structure.

The competitive reaction mechanism was further verified by the variation of reaction rate as influenced by competitor concentration. The dependence of MCAA reduction on bromate concentration over Pd(0.86)/$Ce_{0.8}Zr_{0.2}O_2$ is presented in Fig. 10. The initial activity of Pd(0.86)/$Ce_{0.8}Zr_{0.2}O_2$ for MCAA reduction decreased from 75.2 to 12.7 mM g_{cat}^{-1} h^{-1} when bromate concentration increased from 0 to 0.3 mM. As for the influence of MCAA concentration on bromate reduction, the initial bromate reduction rate decreased by approximately 58% in the presence of 0.3 mM MCAA (see Fig. 10b). The variation of initial MCAA reduction rate as a function of bromate concentration was further fitted to the binary Langmuir–Hinshelwood model:

$$r_{M\,0} = k\theta_{M0} = k\frac{b_M C_{M\,0}}{1 + b_M C_{M\,0} + b_b C_{b\,0}} \quad (3)$$

$$\frac{1}{r_{M\,0}} = \frac{1}{kb_M C_{M\,0}} + \frac{1}{k} + \frac{b_b C_{b\,0}}{kb_M C_{M0}} \quad (4)$$

where r_{M0} is the initial reduction rate of MCAA, C_{M0} is the initial MCAA concentration, C_{b0} is the initial bromate concentration, θ_{M0} is the surface coverage of MCAA adsorption, k is the reaction rate constant, and b_b and b_M are the adsorption constants of bromate and MCAA, respectively.

The plot of $1/r_{M0}$ *versus* C_{b0} gave a good linear relationship with R^2 larger than 0.96, indicating that the simultaneous reduction of bromate and MCAA could be well described using the Langmuir–Hinshelwood model. In parallel, a good linear relationship between $1/r_{b0}$ and C_{M0} was also established (see Fig. 11b), again confirming the competitive reaction mechanism for the simultaneous reduction of bromate and MCAA.

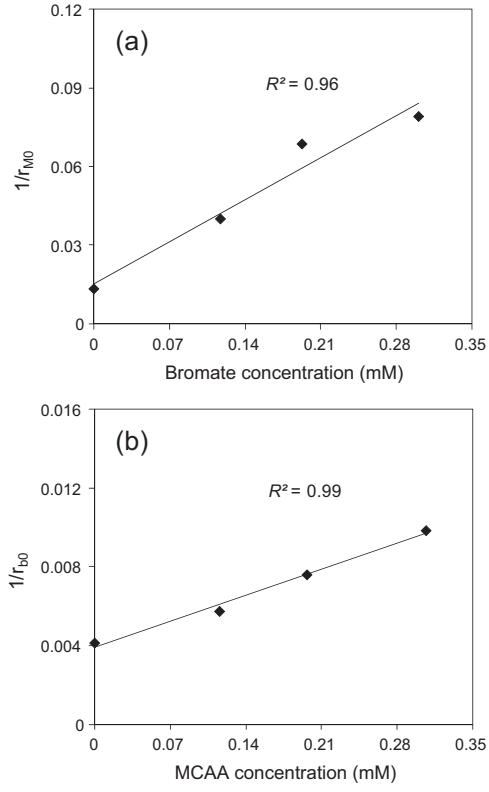

Fig. 11. Linear plots of (a) $1/r_{M0}$ *versus* bromate concentration, and (b) $1/r_{b0}$ *versus* MCAA concentration. Reaction conditions: pH 5.6. Catalyst: Pd(0.86)/$Ce_{0.8}Zr_{0.2}O_2$. Catalyst dosage: 0.033 g l^{-1}.

4. Conclusions

In the present study, a series of Pd catalysts supported on CeO_2, ZrO_2 and $Ce_{1-x}Zr_xO_2$ (x = 0.2, 0.5, 0.8) were prepared, and the individual and simultaneous reduction of bromate and MCAA over the catalysts was investigated. Due to the stronger metal-support interaction, Pd(0.83)/CeO_2 has a higher Pd dispersion than Pd(0.85)/ZrO_2. Accordingly, increasing CeO_2 content results in an increased Pd dispersion in Pd/$Ce_{1-x}Zr_xO_2$, and the maximum Pd dispersion is observed on Pd(0.86)/$Ce_{0.8}Zr_{0.2}O_2$. At a similar Pd loading, Pd/$Ce_{0.8}Zr_{0.2}O_2$ exhibits higher catalytic activities for individual reduction of bromate and MCAA than other catalysts due to more accessible Pd sites and cationization of Pd particles. For Pd/$Ce_{0.8}Zr_{0.2}O_2$ catalysts with varied Pd loadings, the TOF of exposed Pd sites first increases and then keeps constant with Pd particle size, indicative of a more predominant role of H_2 activation for the catalyst with smaller Pd particles. As for simultaneous reduction of MCAA and bromate, bromate exhibits a much stronger reaction competitiveness than MCAA on Pd(0.85)/ZrO_2, whereas enhanced competitiveness of MCAA is observed on Pd(0.86)/$Ce_{0.8}Zr_{0.2}O_2$ in comparison with Pd(0.85)/ZrO_2, and effective and simultaneous reduction of bromate and MCAA can be achieved. Furthermore, the simultaneous reduction of MCAA and bromate on Pd(0.86)/$Ce_{0.8}Zr_{0.2}O_2$ can be well described by the Langmuir–Hinshelwood model, reflecting a competitive adsorption controlled reaction mechanism.

Acknowledgements

The financial support from National Key Basic Research Program of China (2014CB441103) and the National Natural Science Foundation of China (no. 21277066, 21225729 and 21237002) is gratefully acknowledged. We are indebted to the Modern Analytical Center, Nanjing University for the catalyst characterization.

Appendix A. Supplementary data

Supplementary material related to this article can be found, in the online version, at http://dx.doi.org/10.1016/j.apcatb.2014.06.041.

References

[1] P. Westerhoff, P. Chao, H. Mash, Water Res. 38 (2004) 1502–1513.
[2] G.Y. Ding, X.R. Zhang, M.T. Yang, Y. Pan, Water Res. 47 (2013) 2710–2718.
[3] S.D. Richardson, M.J. Plewa, E.D. Wagner, R. Schoeny, D.M. DeMarini, Mutat. Res. 636 (2007) 178–242.
[4] S.K. Golfinopoulos, A.D. Nikolaou, Desalination 176 (2005) 13–24.
[5] H.S. Weinberg, C.A. Delcomyn, V. Unnam, Environ. Sci. Technol. 37 (2003) 3104–3110.
[6] J.A. Pals, J.K. Ang, E.D. Wagner, M.J. Plewa, Environ. Sci. Technol. 45 (2011) 5791–5797.
[7] M.S. Attene-Ramos, E.D. Wagner, M.J. Plewa, Environ. Sci. Technol. 44 (2010) 7206–7212.
[8] H. Kasai, S. Nishimura, Y.J. Kurokawa, Y. Hayashi, Carcinogenesis 8 (1987) 1959–1961.
[9] A.Z. Li, X. Zhao, Y.N. Hou, H.J. Liu, L.Y. Wu, J.H. Qu, Appl. Catal., B: Environ. 111–112 (2012) 628–635.
[10] X.Y. Wang, P. Ning, H.L. Liu, J. Ma, Appl. Catal., B: Environ. 94 (2010) 55–63.
[11] L.L. Lifongo, D.J. Bowden, P. Brimblecombe, Chemosphere 55 (2004) 467–476.
[12] Q.L. Wang, S. Snyder, J. Kim, H. Choi, Environ. Sci. Technol. 43 (2009) 3292–3299.
[13] F.M.M. Paschoal, G. Pepping, M.V.B. Zanoni, M.A. Anderson, Environ. Sci. Technol. 43 (2009) 7496–7502.
[14] H. Chen, Z.Y. Xu, H.Q. Wan, J.Z. Zheng, D.Q. Yin, S.R. Zheng, Appl. Catal., B: Environ. 96 (2010) 307–313.
[15] P. Zhang, F. Jiang, H. Chen, Chem. Eng. J. 234 (2013) 195–202.
[16] J. Zhou, Y.X. Han, W.J. Wang, Z.Y. Xu, H.Q. Wan, D.Q. Yin, S.R. Zheng, D.Q. Zhu, Appl. Catal., B: Environ. 134–135 (2013) 222–230.
[17] P.S.S. Reddy, N. Pasha, M.G.V.C. Rao, N. Lingaiah, I. Suryanarayana, P.S.S. Prasad, Catal. Commun. 8 (2007) 1406–1410.
[18] R. Gopinath, N.S. Babu, J.V. Kumar, N. Lingaiah, P.S.S. Prasad, Catal. Lett. 120 (2008) 312–319.
[19] L.M.T. Martinez, M. Araque, J.C. Vargas, A.C. Roger, Appl. Catal., B: Environ. 132–133 (2013) 499–510.
[20] R. Sadiq, M.J. Rodriguez, Sci. Total Environ. 321 (2004) 21–46.
[21] G. Yuan, M.A. Keane, Ind. Eng. Chem. Res. 46 (2007) 705–715.
[22] G. Yuan, M.A. Keane, Chem. Eng. Sci. 58 (2003) 257–267.
[23] G. Agostini, R. Pellegrini, G. Leofanti, L. Bertinetti, S. Bertarione, E. Groppo, A. Zecchina, C. Lamberti, J. Phys. Chem. C 113 (2009) 10485–10492.
[24] E. Groppo, G. Agostini, A. Piovano, N.B. Muddada, G. Leofanti, R. Pellegrini, G. Portale, A. Longo, C. Lamberti, J. Catal. 287 (2012) 44–54.
[25] K. Bourikas, J. Vakros, C. Kordulis, A. Lycourghiotis, J. Phys. Chem. B 107 (2003) 9441–9451.
[26] J. Vakros, C. Kordulis, A. Lycourghiotis, Chem. Commun. (2002) 1980–1981.
[27] W.Z. Li, H. Huang, H.J. Li, W. Zhang, H.C. Liu, Langmuir 24 (2008) 8358–8366.
[28] D.R. Burri, K.M. Choi, J.H. Lee, D.S. Han, S.E. Park, Catal. Commun. 8 (2007) 43–48.
[29] P. Bera, K.C. Patil, V. Jayaram, G.N. Subbanna, M.S. Hegde, J. Catal. 196 (2000) 293–301.
[30] K.R. Priolkar, P. Bera, P.R. Sarode, M.S. Hegde, S. Emura, R. Kumashiro, N.P. Lalla, Chem. Mater. 14 (2002) 2120–2128.
[31] P.S. Querino, J.R.C. Bispo, M.C. Rangel, Catal. Today 107–108 (2005) 920–925.
[32] F. Vindigni, M. Manzoli, T. Tabakova, V. Idakiev, F. Boccuzzi, A. Chiorino, Appl. Catal., B: Environ. 125 (2012) 507–515.
[33] L.F. Liotta, G.D. Carlo, G. Pantaleo, A.M. Venezia, Catal. Today 158 (2010) 56–62.
[34] W.C.J. Wei, S.C. Wang, F.Y. Ho, J. Am. Ceram. Soc. 82 (1999) 3385–3392.
[35] J. Wang, L. Gao, Nanostruct. Mater. 11 (1999) 451–457.
[36] D. Briggs, Practical surface analysis, in: M.P. Seah (Ed.), Auger and X-ray Photoelectron Spectroscopy, vol.1, second ed., Wiley, New York, NY, 1990.
[37] C.D. Wagner, A.V. Naumkin, A. Kraut-Vass, J.W. Allison, C.J. Powell, J.R. Rumble, X-ray Photoelectron Spectroscopy Database, National Institute of Standard and Technology (NIST) Technology Services, United States of America, 2007.
[38] W.J. Shen, M. Okumura, Y. Matsumura, M. Haruta, Appl. Catal., A: Gen. 213 (2001) 225–232.
[39] E. Mamontov, T. Egami, R. Brezny, M. Koranne, S. Tyagi, J. Phys. Chem. B 104 (2000) 11110–11116.
[40] J.A. Farmer, C.T. Campbell, Science 329 (2010) 933–936.
[41] A. Sepulveda-Escribano, F. Coloma, F. Rodriguez-Reinoso, J. Catal. 178 (1998) 649–657.
[42] Y. Shao, Z.Y. Xu, H.Q. Wan, Y.Q. Wan, H. Chen, S.R. Zheng, D.Q. Zhu, Catal. Commun. 12 (2011) 1405–1409.
[43] J. Zhou, K. Wu, W.J. Wang, Z.Y. Xu, H.Q. Wan, S.R. Zheng, Appl. Catal., A: Gen. 470 (2014) 336–343.
[44] Y. Nagai, K. Dohmae, Y. Ikeda, N. Takagi, N. Hara, T. Tanabe, G. Guilera, S. Pascarelli, M.A. Newton, N. Takahashi, H. Shinjoh, S. Matsumoto, Catal. Today 175 (2011) 133–140.
[45] J.A. Baeza, L. Calvo, M.A. Gilarranz, A.F. Mohedano, J.A. Casas, J.J. Rodriguez, J. Catal. 293 (2012) 85–93.
[46] L.M. Gomez-Sainero, X.L. Seoane, J.L.G. Fierro, A. Arcoya, J. Catal. 209 (2002) 279–288.
[47] A. Pintar, J. Batista, J. Levec, T. Kajiuchi, Appl. Catal., B: Environ. 11 (1996) 81–98.
[48] Z.M. de Pedro, J.A. Casas, L.M. Gomez-Sainero, J.J. Rodriguez, Appl. Catal., B: Environ. 98 (2010) 79–85.
[49] T. Zhang, J.P. Croue, Appl. Catal., B: Environ. 144 (2014) 831–839.
[50] K. Groenen-Serrano, E. Weiss-Hortala, A. Savall, P. Spiteri, Electrocatalysis 4 (2013) 346–352.
[51] J.M. Moreno, M.A. Aramendia, A. Marinas, J.M. Marinas, F.J. Urbano, Appl. Catal., B: Environ. 76 (2007) 34–41.